COLD SPRING HARBOR
Molecular Case Studies

RESEARCH REPORT

Clonal dynamics of donor-derived myelodysplastic syndrome after unrelated hematopoietic cell transplantation for high-risk pediatric B-lymphoblastic leukemia

Jason R. Schwartz,[1,5] Michael P. Walsh,[2,5] Jing Ma,[2] Tamara Lamprecht,[2] Shuoguo Wang,[3] Gang Wu,[3] Susana Raimondi,[2] Brandon M. Triplett,[4] and Jeffery M. Klco[2]

[1]Department of Oncology, St. Jude Children's Research Hospital, Memphis, Tennessee 38105, USA; [2]Department of Pathology, St. Jude Children's Research Hospital, Memphis, Tennessee 38105, USA; [3]Department of Computational Biology, St. Jude Children's Research Hospital, Memphis, Tennessee 38105, USA; [4]Department of Bone Marrow Transplant & Cellular Therapy, St. Jude Children's Research Hospital, Memphis, Tennessee 38105, USA

Abstract Donor-derived hematologic malignancies are rare complications of hematopoietic cell transplantation (HCT). Although these are commonly either a myelodysplastic syndrome (MDS) or acute myeloid leukemia (AML), in general, they are a heterogeneous group of diseases, and a unified mechanism for their development has remained elusive. Here we report next-generation sequencing, including whole-exome sequencing (WES), whole-genome sequencing (WGS), and targeted sequencing, of a case of donor-derived MDS (dMDS) following HCT for high-risk B-lymphoblastic leukemia (B-ALL) in an adolescent. Through interrogation of single-nucleotide polymorphisms (SNPs) in the WGS data, we unequivocally prove that the MDS is donor-derived. Additionally, we sequenced 15 samples from 12 time points, including the initial B-ALL diagnostic sample through several post-HCT remission samples, the dMDS, and representative germline samples from both patient and donor, to show that the MDS-related pathologic mutations, including a canonical *ASXL1* (p.Y700*) mutation, were detectable nearly 3 yr prior to the morphological detection of MDS. Furthermore, these MDS mutations were not detectable immediately following, and for >1 yr post-, HCT. These data support the clinical utility of comprehensive sequencing following HCT to detect donor-derived malignancies, while providing insights into the clonal progression of dMDS over a 4-yr period.

[Supplemental material is available for this article.]

Corresponding authors:
Jeffery.Klco@STJUDE.ORG;
Brandon.Triplett@STJUDE.ORG

Ontology terms: leukemia; multiple lineage myelodysplasia

Published by Cold Spring Harbor Laboratory Press

doi: 10.1101/mcs.a002980

INTRODUCTION

Donor-derived hematologic malignancies are rare complications of hematopoietic cell transplantation (HCT) with an incidence of ~0.1% (Kato et al. 2016). However, donor-derived neoplasms may range as high as 5% given the potential for underestimation due to the historic

[5]These authors contributed equally to this work.

limitation of unequivocally demonstrating donor origin (Wiseman 2011). The first published report of a donor-derived hematologic malignancy was in 1971 (Goh et al. 1971), and following this first case, several case reports, series, and retrospective surveys have documented less than 150 cases (Shiozaki et al. 2014; Kato et al. 2016). Infections and other diseases, such as autoimmune disorders (Niederwieser et al. 2004) or hematologic malignancy, have been shown to be transmitted from the donor, and in some cases these diseases have been proven to be present at the time of transplantation (Dias et al. 2017), whereas in others the donors remain well without evidence of disease (Wiseman 2011; Fiala et al. 2015). Several mechanisms for the development of donor-derived malignancy have been proposed and comprehensively reviewed (Wiseman 2011), but a consolidated hypothesis remains elusive given the heterogeneity of the cases reported to date. This heterogeneity is evident in two recent studies of donor-derived hematological malignancies. In one study, a *TET2* mutation was identified as the founding lesion of a recipient's donor-derived myelodysplastic syndrome (MDS) that originated from the donor's clonal hematopoiesis of indeterminate potential (CHIP) (Rojek et al. 2016). In a second study, a donor-derived AML with a *NPM1* mutation was only present in the recipient, whereas the donor reportedly remains without mutation and clinically well (Rodríguez-Macías et al. 2013).

Here we describe, with comprehensive next-generation sequencing, the clonal dynamics of a donor-derived MDS in a young adult with monosomy 7 and a loss of function *ASXL1* mutation.

Clinical Presentation and Course

A 15-yr-old male presented for medical attention because of chronic headaches; his laboratory workup revealed leukocytosis (WBC: 130,000/mm^3) and thrombocytopenia (platelets: 113,000/mm^3). Diagnostic bone marrow studies revealed 90% blasts by morphology with an immunophenotype consistent with B-lymphoblastic leukemia (B-ALL). Conventional karyotyping showed an abnormal karyotype—46,XY, t(2;9)(q21;q34) [14]; 46,XY [6]—and fluorescence in situ hybridization (FISH) studies demonstrated an *ABL1* fusion. The patient started induction therapy with a seven-drug regimen on a Total Therapy for Leukemia protocol (Pui et al. 2009). Following induction and consolidation therapy, the patient's minimal residual disease (MRD) remained positive; therefore, he received reintensification therapy in preparation for HCT. The patient's MRD remained positive at a low level until after HCT (Fig. 1A). He received a matched (7/8) unrelated donor transplant from a 43-yr-old female donor. His pretransplant conditioning regimen included myeloablative total body irradiation, cyclophosphamide, thiotepa, and antithymocyte globulin (ATG). Following transplant, the patient had many transplant-related morbidities including acute, and later chronic, graft versus host disease of the skin, gut, and liver, chronic lung disease, and chronic renal failure due to BK virus nephropathy requiring intermittent dialysis. Forty-four months after his initial leukemia diagnosis, an incidentally found left renal mass was confirmed to be renal cell carcinoma (RCC) positive for a Xp11.2 lesion with a *ASPSCR1-TFE3* fusion transcript; he was treated with a left nephrectomy. Eleven months following the left RCC diagnosis, the patient was diagnosed with a right RCC with the Xp11.2 alteration but no *ASPSCR1-TFE3* fusion. Therefore, the right RCC was determined to represent a second primary tumor also treated with a nephrectomy, leaving the patient anephric and dialysis-dependent. Five months following the second RCC, the patient developed a lower lip lesion that was diagnosed as squamous cell carcinoma (SCC) and surgically excised. At 5.5 yr following the patient's initial B-ALL diagnosis (4 yr post-HCT), the patient was diagnosed with MDS following a routine annual bone marrow evaluation demonstrating multilineage dysplasia and an abnormal karyotype, including monosomy 7 (Fig. 1B,C). Molecular analyses of the patient's marrow samples showed 100% chimerism, which was further supported by FISH for Chromosome X,

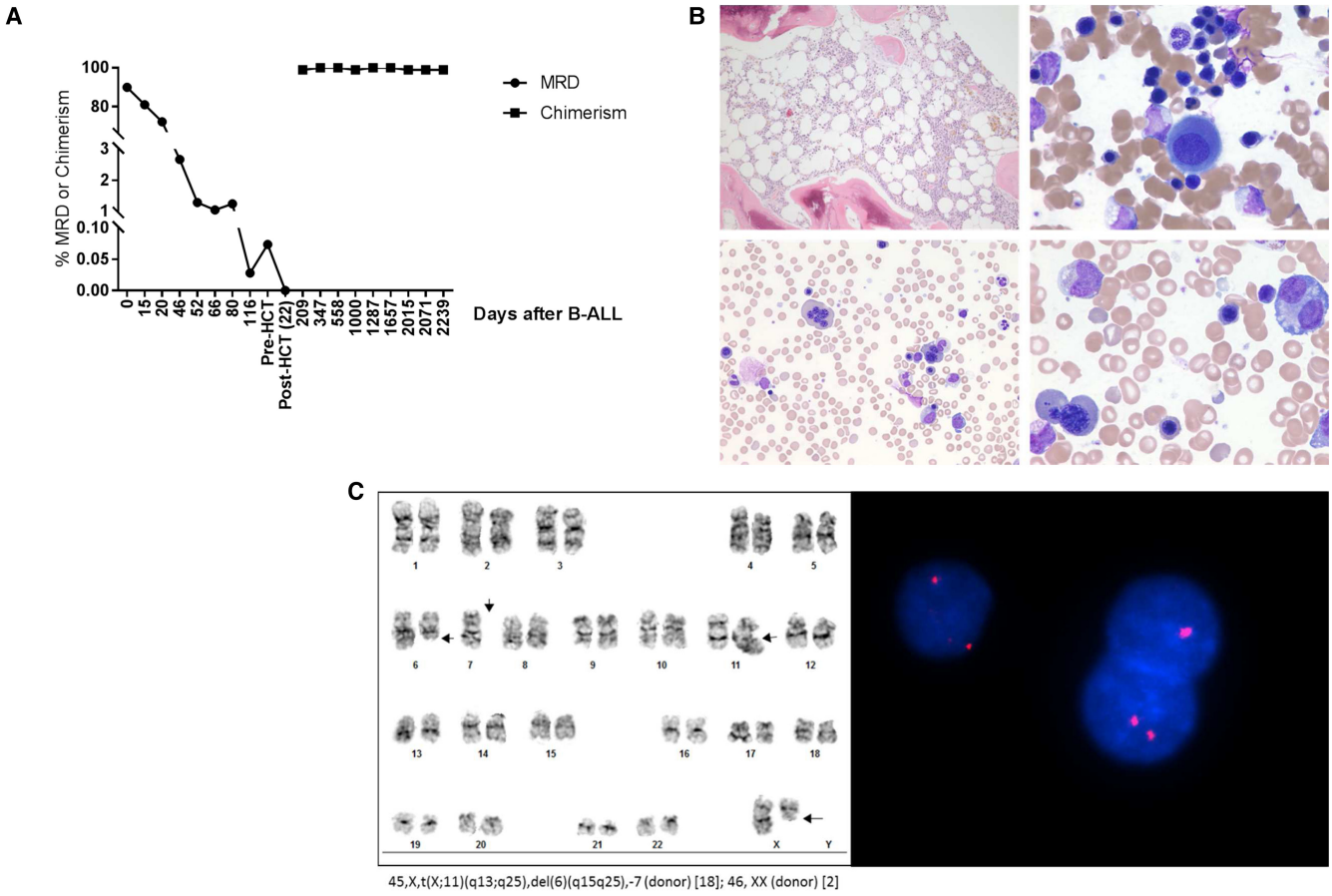

Figure 1. Clinical and response characteristics of dMDS. (*A*) MRD, as measured by flow cytometric analysis of the leukemia-associated immunophenotype or chimerism (VNTR PCR analysis), levels at listed time after initial B-ALL diagnosis. (*B*) Morphologic evaluation of the bone marrow biopsy and aspirate at the time of dMDS diagnosis showing hypocellularity and dysplastic changes. (*C*) Conventional karyotype (*left* panel) of the MDS sample demonstrating partial deletion of Chromosomes 6 and monosomy 7 and XY FISH (*right* panel) showing only X chromosomes (red probe) and the absence of Y, consistent with donor origin.

suggesting that the MDS is donor-derived (dMDS). Subsequently, his peripheral counts were monitored frequently as he became transfusion-dependent. Intermittent bone marrow evaluations never showed progression to AML. One year following the MDS diagnosis, the patient developed another lip lesion (upper lip) that was confirmed to be SCC with significant local invasion. No additional therapy was pursued. Three months later imaging confirmed the development of several metastatic pulmonary nodules, and he succumbed to his diseases one month later following an episode of pneumonia.

Genomic Analysis

Twelve distinct samples were available for genomic interrogation from this patient as part of an institutional IRB-approved protocol for the collection and genomic analysis of patient samples following informed consent. These samples provide an opportunity to comprehensively follow the clonal dynamics of this patient's presumed donor-derived MDS. This includes three pretransplant samples, including his original diagnostic B-ALL, as well as nine posttransplant samples (Supplemental Table 1). Although material directly from his allograft

was not available, we did have access to a sample collected from his bone marrow 22 d after the allograft, at which time clinical testing showed 99% donor engraftment. In addition, purified lymphocytes were obtained by flow cytometry as a source of "germline" genomic DNA, and bone marrow fibroblasts/stromal cells were cultured to provide an additional source of the patient's germline. Whole-exome sequencing (Illumina Nextera Rapid Capture Expanded Exome, 62 Mb) and whole-genome sequencing (WGS) were performed on the MDS sample (Supplemental Tables 2–4). The diagnostic ALL was characterized by WGS. Using this information, we also established a targeted panel (Haloplex, Agilent Technologies) to follow five variants in the B-ALL and 28 in the MDS as well as 11 single-nucleotide polymorphisms (SNPs) to distinguish the donor and patient/recipient (Fig. 2A,B; Supplemental Tables 5–9).

First, we unequivocally demonstrate that the MDS is derived from the donor by tracking SNPs that distinguish the donor and recipient cells (Fig. 2A). These data clearly show that the genotype of the MDS is consistent with donor cells. In addition, our sequencing of the B-ALL and dMDS samples show neoplasms with dramatically different mutational profiles. The B-ALL sample has a complex rearrangement of Chromosomes 2, 9, and 15 that involves *ABL1*, consistent with a Ph-like ALL, as well as a *CREBBP* splice site mutation involving exon 21. These alterations were not present in the MDS. In contrast, the MDS sample from day 2071 has 47 somatic alterations (32 missense, 1 nonsense, 11 silent, and 3 splice region mutations), including a nonsense mutation in *ASXL1* (c.T2100A; p.Y700*) at a variant allele frequency (VAF) of 0.46 (WES) (Table 1). Although *ASXL1* mutations are common in adult MDS (Haferlach et al. 2014), they are less common in pediatric MDS (Pastor et al. 2017; Schwartz et al. 2017a). We also confirmed the monosomy 7, as well as a focal deletion of Chromosome 6 (Fig. 2C). We then sequenced all 12 samples using the targeted panel (average median coverage 534×) to determine when the *ASXL1* variant and 27 other somatic mutations identified in the MDS sample were present relative to the transplant and the diagnosis of MDS. The median VAF for the 28 dMDS variants first rose above 2% at day 1657, which is 1470 d after the bone marrow transplant and 358 d prior to any morphologic evidence of dysplasia (Fig. 2D). Specifically, the *ASXL1* variant was first detected at a VAF >2% at day 1657, although supporting reads were first present at day 1000. We used allele-specific droplet digital PCR to confirm the presence of *ASXL1* mutant alleles as early as Day 1000. Moreover, we show that this variant is not detectable until day 1000 (813 d after HCT) with a steady increase after that time (Fig. 2E; Supplemental Fig. 2). In contrast, although we could detect low levels of the *CREBBP* mutation in the patient's B-ALL at day 66 (Supplemental Fig. 1), this mutation was not present at any later time point, including the post-transplant MDS samples. Despite the presence of multiple cancers in the recipient, WGS analysis did not identify any obvious disease-causing germline variants in genes commonly implicated in cancer predisposition syndromes (Supplemental Tables 10, 11), nor were any germline variants in MDS/AML genes present in the donor. In silico predictions scored a novel *TOP2B* variant as the most deleterious (CADD score: 35) variant in the patient's germline (http://cadd.gs.washington.edu/info)(Kircher et al. 2014). Although *TOP2B* alterations have been implicated in both de novo and therapy-related AML (Nebral et al. 2005; Smith et al. 2014), the significance of this variant in this context is uncertain.

DISCUSSION

The development of a myeloid neoplasm arising from cells of donor origin following HCT could result from unknowingly transferring cells that harbor germline mutations or cells that have acquired mutations associated with clonal hematopoiesis (e.g., *TET2* [Rojek et al. 2016] or *DNMT3A* [Yasuda et al. 2014]). *ASXL1* variants are commonly observed in

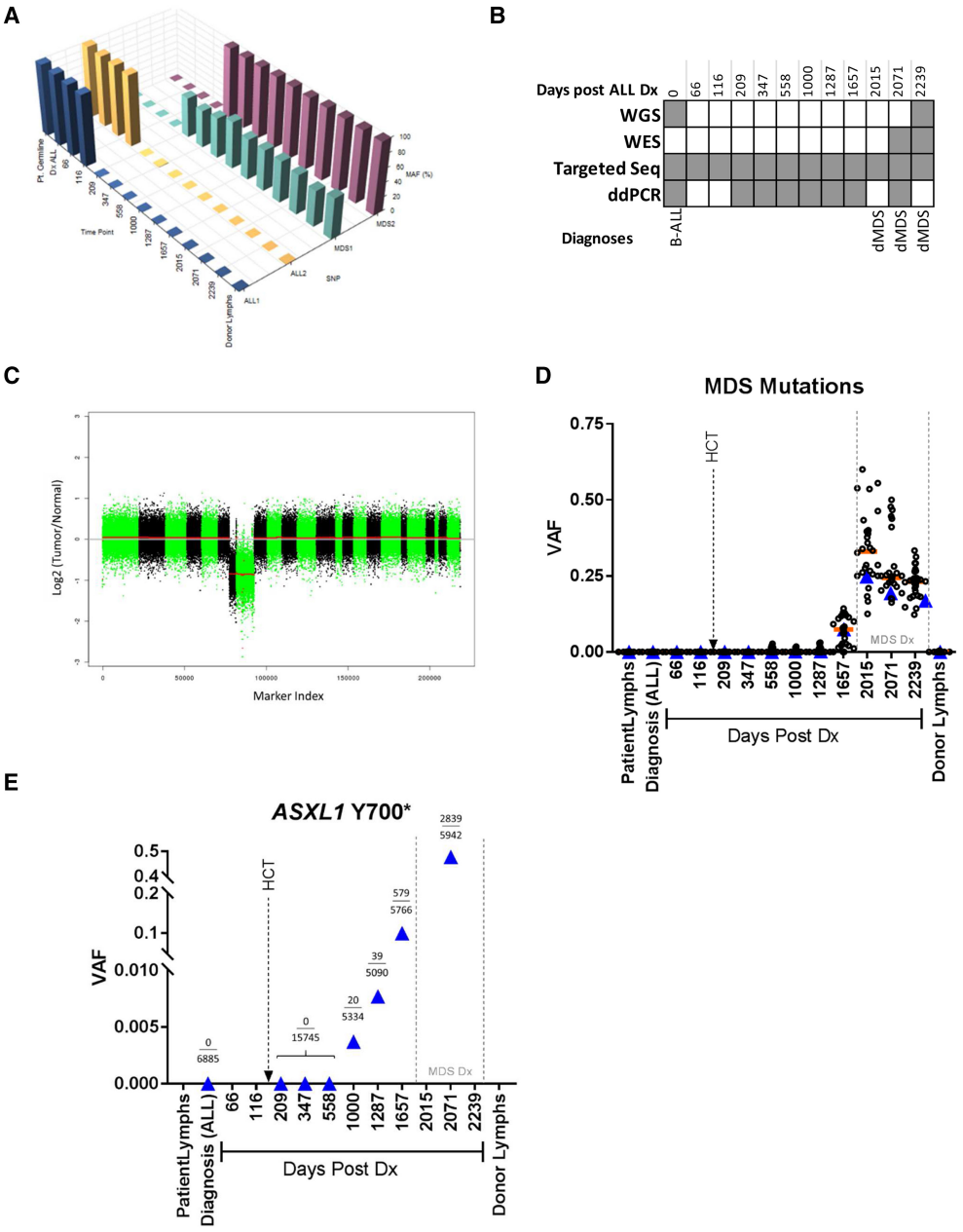

Figure 2. Clonal dynamics of dMDS. (*A*) Minor allele frequencies (MAF) of SNPs unique to patient (ALL1 & ALL2) and donor (MDS1 & MDS2) at various time points. Patient-specific SNPs are only present prior to transplant and donor-specific SNP only after transplant. (*B*) Chart demonstrating the sequencing approach used for each sample at each time point. (*C*) Copy number analysis from WES data for the dMDS sample showing monosomies of Chromosomes 6 and 7. The chromosomes are arranged *left* to *right* (Chr1 on the far *left*), and odd chromosomes are highlighted in green and even chromosomes in black. (*D*) VAF timeline of pathologic mutations identified in the dMDS via targeted sequencing (HaloPlex). The Day 2071 sample was a sorted myeloid population versus a bulk marrow population as in the other time points; therefore, the values shown are corrected by a factor of 2 given that the lymphocyte population comprised 50% of that initial bulk population. (*E*) VAF timeline of *ASXL1* Y700* mutation identified in the dMDS via allele-specific droplet digital PCR. Absolute read counts for the mutant allele (numerator) and total reads (denominator) are listed. Notes for *D*,*E*: The *ASXL1* mutation is denoted by the blue triangle. The vertical gray hatched lines demarcate the time when morphologic evidence of MDS is present. The orange lines demonstrate the median VAF for the time point.

Table 1. Significant sequence variant identified in donor-derived myelodysplastic syndrome

Gene	Chr: position GRCh37 (hg19)	HGVS DNA reference	HGVS protein reference	Variant type	Predicted effect	Genotype
ASXL1	Chr 20: 31022615	c.2100T>A	p. Tyr700Stop	Nonsense substitution	Loss of function	Somatic heterozygous

patients with CHIP (Jaiswal et al. 2014). Considering the high VAF of the *ASXL1* variant observed for this donor-derived MDS, the most likely explanation in this case is that a rare hematopoietic stem and progenitor cell (HSPC) with the *ASXL1* p.Y700* mutation was unknowingly transferred to the recipient during HCT. However, our digital droplet PCR data show that the variant was not detectable until 813 d after the HCT, suggesting that this mutation potentially arose after the HCT. Further, CHIP is uncommon in individuals in their 40s (Jaiswal et al. 2014; Babushok et al. 2016). However, even the most sensitive sequencing techniques cannot completely rule out that a preexisting mutation in a rare HSPC was transferred from the donor. Alternatively, the donor-derived MDS in this case could have resulted in the recipient as a result of cell extrinsic pressures, such as microenvironmental stresses (Greenberger et al. 1996; Flores-Figueroa et al. 2002; Raaijmakers et al. 2010), including damaging stromal mutations, residual effects of cytotoxic chemotherapy, radiation bystander effects, or impaired immune surveillance (Wiseman 2011). Although no definitive germline variants linked to cancer predisposition were identified in this patient by WGS, the presence of multiple malignancies does suggest a potential permissive environment. Likewise, dMDS has been reported in a recipient with Fanconi anemia (Gustafsson et al. 2012). To our knowledge, the donor remains healthy without clinical symptoms (e.g., peripheral cytopenias). Like previously reported cases, this patient developed monosomy 7 and received hematopoietic growth factors (in our case erythropoietin) prior to developing dMDS, though none of the previously reported cases had ALL as the initial diagnosis (Dietz et al. 2014). In addition to providing critical insights into the clonal progression of donor-derived MDS, our data also demonstrate the utility of sequencing approaches in the diagnosis of myeloid neoplasms after HCT, as we detected MDS-related mutations nearly 3 yr prior to a morphologic diagnosis.

METHODS

MRD was measured by flow cytometry and defined as negative when the leukemia-associated immunophenotype was expressed on <0.01% of bone marrow mononucleated cells. Post-HCT chimerism was measured via variable number of tandem repeats (VNTR) PCR analysis. Whole-genome, whole-exome, and targeted amplicon sequencing and analyses were completed on samples paired with flow-sorted lymphocytes (as a source of germline genomic DNA) as previously described (Schwartz et al. 2017a,b). Patient fibroblasts were cultured from the banked dMDS sample (Day 2239). Analysis of WGS and WES data, which include mapping, coverage, and quality assessment, SNV/indel detection, tier annotation for sequence mutations, prediction of deleterious effects of missense mutations, and identification of loss of heterozygosity, were described previously (Zhang et al. 2012). The detection and annotation of germline variants were performed by a workflow named "medal ceremony" described previously (Zhang et al. 2015). Coverage data and statistics are documented in Supplemental Table 12. The mean coverage for WES and WGS was 86× and 52×, respectively. Pair-end reads of an average length of 100 and 151 were obtained for WES and WGS, respectively. Single-nucleotide variations (SNVs) were classified into the following four tiers: tier 1, coding synonymous, nonsynonymous, splice site, and

noncoding RNA variants; tier 2, conserved variants (cutoff: conservation score greater than or equal to 500 based on either the phastConsElements28way table or the phastConsElements17way table from the UCSC genome browser) and variants in regulatory regions annotated by UCSC annotation (regulatory annotations included are targetScanS, ORegAnno, tfbsConsSites, vistaEnhancers,eponine, firstEF, L1 TAF1 Valid, Poly(A), switchDbTss, encodeUViennaRnaz, laminB1, cpgIslandExt); tier 3, variants in nonrepeat masked regions; and tier 4, the remaining variants. Structural variations in WGS were analyzed using CREST (Wang et al. 2011). For copy-number analysis, SAMtools (Li et al. 2009) mpileup command was used to generate an mpileup file from matched normal and tumor BAM files with duplicates removed. VarScan2 was then used to take the mpileup file to call somatic CNAs after adjusting for normal/tumor sample read coverage depth and GC content. Circular Binary Segmentation algorithm (Olshen et al. 2004) implemented in the DNAcopy R package was used to identify the candidate CNAs for each sample. B-allele frequency info for all high-quality dbSNPs heterozygous in the germline sample was also used to assess allele imbalance. For Haloplex analysis, samples were aligned and SNVs were called using Agilent SureCall software (*Agilent HaloPlex Target Enrichment: Design and Analysis of Clinical Research Panels,* Publication number 5991-1919EN). The software merges duplicate sequencing reads into single reads using a molecular barcode system, and the number of merged reads is recorded in the resulting bam file. Using these numbers, absolute read count coverage for every SNV was calculated. In some instances, reads collapsed from a single barcode (reads that were not duplicated) were excluded from the analysis. All read counts were performed using the pysam module (https://github.com/pysam-developers/pysam) of the Python computing language (http://www.python.org/). The average median read depth for the 12 samples analyzed by targeted sequencing (Haloplex) was 534×. Allele-specific droplet digital PCR was performed on 25 ng of template gDNA using TaqMan Genotyping Master Mix (Applied Biosystems) and custom *ASXL1* TaqMan (Thermo-Fisher) primers and probes [5′-TCTACAGCGAACACAACTACTGC (forward), 5′-TCCGGCCTGGGTATGCT (reverse), 5′-VIC-CATTTAGAGGATAAGGCG (wild-type), 5′-FAM-CCATTTAGAGGTTAAGGCG (mutant)]. Droplets were generated using the RainDance Source instrument and amplification was performed with the following conditions: 10 min at 95°C, 40 cycles of 95°C for 30 sec, 60°C for 1 min. Fluorescence of the amplified droplets was detected by the RainDance Sense instrument and the resulting data was analyzed using RainDrop Analyst II software.

ADDITIONAL INFORMATION

Data Deposition and Access

DNA sequencing data are deposited to the European Genome-phenome Archive (EGA; www.ebi.ac.uk/ega/home) under accession EGAS00001002202. The *ASXL1* p.Y700* variant was submitted to ClinVar (http://www.ncbi.nlm.nih.gov/clinvar/) and can be found under accession number SCV000778455.

Ethics Statement

Bone marrow samples were banked for research after informed consent was obtained under an institutional biorepository protocol allowing for whole-genome testing, germline testing, and deposition into genomic databases. Further, written and verbal informed consent specific to this study was also obtained from the patient's family. These studies were approved by the Institutional Review Board at St. Jude Children's Research Hospital.

Acknowledgments

We thank this patient and family and clinical staff involved in his care. We thank the Biorepository, the Flow Cytometry and Cell Sorting Core at St Jude Children's Research Hospital, and the Hartwell Center for Bioinformatics and Biotechnology of St. Jude Children's Research Hospital. Jinghui Zhang and the Department of Computational Biology graciously provided previously established bioinformatic pipelines and support.

Author Contributions

J.R.S., M.P.W, J.M., T.L., G.W., S.W., and J.M.K. contributed to experimental design and data analysis. B.M.T. assisted with clinical information regarding this patient. J.R.S. and J.M.K. prepared the manuscript.

Competing Interest Statement

The authors have declared no competing interest.

Received March 9, 2018; accepted in revised form May 29, 2018.

Funding

This work was funded by the American Lebanese and Syrian Associated Charities of St. Jude Children's Research Hospital and grants from the U.S. National Institutes of Health-P30 CA021765, Cancer Center Support Grant and K08 HL116605 (J.M.K.). J.M.K. holds a Career Award for Medical Scientists from the Burroughs Wellcome Fund and a Scholar Award from the V Foundation.

REFERENCES

Babushok DV, Bessler M, Olson TS. 2016. Genetic predisposition to myelodysplastic syndrome and acute myeloid leukemia in children and young adults. *Leuk Lymphoma* **57:** 520–536.

Dias A, Al-Kali A, Van Dyke D, Niederwieser D, Vucinic V, Lemke J, Muller C, Schwind S, Teichmann AC, Bakken R, et al. 2017. Inversion 3 cytogenetic abnormality in an allogeneic hematopoietic cell transplant recipient representative of a donor-derived constitutional abnormality. *Biol Blood Marrow Transplant* **23:** 1582–1587.

Dietz AC, DeFor TE, Brunstein CG, Wagner JE Jr. 2014. Donor-derived myelodysplastic syndrome and acute leukaemia after allogeneic haematopoietic stem cell transplantation: incidence, natural history and treatment response. *Br J Haematol* **166:** 209–212.

Fiala M, Hucthagowder V, Westervelt P, Stockerl-Goldstein K, Kulkarni S, Ghobadi A. 2015. Two cases of donor-derived malignancies following allogeneic hematopoietic stem cell transplantation. *Ann Hematol Oncol* **2:** 1051–1053.

Flores-Figueroa E, Gutiérrez-Espindola G, Montesinos JJ, Arana-Trejo RM, Mayani H. 2002. In vitro characterization of hematopoietic microenvironment cells from patients with myelodysplastic syndrome. *Leuk Res* **26:** 677–686.

Goh K, Fialkow PJ, Thomas ED, Bryant JI, Neiman PE. 1971. Leukaemic transformation of engrafted human cells in vivo. *Lancet* **2:** 101–102.

Greenberger JS, Anderson J, Berry LA, Epperly M, Cronkite EP, Boggs SS. 1996. Effects of irradiation of CBA/Ca mice on hematopoietic stem cells and stromal cells in long-term bone marrow cultures. *Leukemia* **10:** 514–527.

Gustafsson B, Moell J, Leblanc K, Barbany G, Soderhäll S, Winiarski J. 2012. Donor cell-derived acute myeloid leukemia after second allogenic cord blood transplantation in a patient with Fanconi anemia. *Pediatr Transplant* **16:** E241–E245.

Haferlach T, Nagata Y, Grossmann V, Okuno Y, Bacher U, Nagae G, Schnittger S, Sanada M, Kon A, Alpermann T, et al. 2014. Landscape of genetic lesions in 944 patients with myelodysplastic syndromes. *Leukemia* **28:** 241–247.

Jaiswal S, Fontanillas P, Flannick J, Manning A, Grauman PV, Mar BG, Lindsley RC, Mermel CH, Burtt N, Chavez A, et al. 2014. Age-related clonal hematopoiesis associated with adverse outcomes. *N Engl J Med* **371:** 2488–2498.

Kato M, Yamashita T, Suzuki R, Matsumoto K, Nishimori H, Takahashi S, Iwato K, Nakaseko C, Kondo T, Imada K, et al. 2016. Donor cell–derived hematological malignancy: a survey by the Japan Society for Hematopoietic Cell Transplantation. *Leukemia* **30:** 1742–1745.

Kircher M, Witten DM, Jain P, O'Roak BJ, Cooper GM, Shendure J. 2014. A general framework for estimating the relative pathogenicity of human genetic variants. *Nat Genet* **46:** 310–315.

Li H, Handsaker B, Wysoker A, Fennell T, Ruan J, Homer N, Marth G, Abecasis G, Durbin R; 1000 Genome Project Data Processing Subgroup. 2009. The Sequence Alignment/Map format and SAMtools. *Bioinformatics* **25:** 2078–2079.

Nebral K, Schmidt HH, Haas OA, Strehl S. 2005. *NUP98* is fused to topoisomerase (DNA) IIβ 180 kDa (*TOP2B*) in a patient with acute myeloid leukemia with a new t(3;11)(p24;p15). *Clin Cancer Res* **11:** 6489–6494.

Niederwieser D, Gentilini C, Hegenbart U, Lange T, Moosmann P, Pönisch W, Al-Ali H, Raida M, Ljungman P, Tyndall A, et al. 2004. Transmission of donor illness by stem cell transplantation: should screening be different in older donors? *Bone Marrow Transplant* **34:** 657–665.

Olshen AB, Venkatraman ES, Lucito R, Wigler M. 2004. Circular binary segmentation for the analysis of array-based DNA copy number data. *Biostatistics* **5:** 557–572.

Pastor V, Hirabayashi S, Karow A, Wehrle J, Kozyra EJ, Nienhold R, Ruzaike G, Lebrecht D, Yoshimi A, Niewisch M, et al. 2017. Mutational landscape in children with myelodysplastic syndromes is distinct from adults: specific somatic drivers and novel germline variants. *Leukemia* **31:** 759–762.

Pui CH, Campana D, Pei D, Bowman WP, Sandlund JT, Kaste SC, Ribeiro RC, Rubnitz JE, Raimondi SC, Onciu M, et al. 2009. Treating childhood acute lymphoblastic leukemia without cranial irradiation. *N Engl J Med* **360:** 2730–2741.

Raaijmakers MH, Mukherjee S, Guo S, Zhang S, Kobayashi T, Schoonmaker JA, Ebert BL, Al-Shahrour F, Hasserjian RP, Scadden EO, et al. 2010. Bone progenitor dysfunction induces myelodysplasia and secondary leukaemia. *Nature* **464:** 852–857.

Rodríguez-Macías G, Martínez-Laperche C, Gayoso J, Noriega V, Serrano D, Balsalobre P, Muñoz-Martínez C, Díez-Martín JL, Buño I. 2013. Mutation of the *NPM1* gene contributes to the development of donor cell-derived acute myeloid leukemia after unrelated cord blood transplantation for acute lymphoblastic leukemia. *Hum Pathol* **44:** 1696–1699.

Rojek K, Nickels E, Neistadt B, Marquez R, Wickrema A, Artz A, van Besien K, Larson RA, Lee MK, Segal JP, et al. 2016. Identifying inherited and acquired genetic factors involved in poor stem cell mobilization and donor-derived malignancy. *Biol Blood Marrow Transplant* **22:** 2100–2103.

Schwartz JR, Ma J, Lamprecht T, Walsh M, Wang S, Bryant V, Song G, Wu G, Easton J, Kesserwan C, et al. 2017a. The genomic landscape of pediatric myelodysplastic syndromes. *Nat Commun* **8:** 1557.

Schwartz JR, Wang S, Ma J, Lamprecht T, Walsh M, Song G, Raimondi SC, Wu G, Walsh MF, McGee RB, et al. 2017b. Germline SAMD9 mutation in siblings with monosomy 7 and myelodysplastic syndrome. *Leukemia* **31:** 1827–1830.

Shiozaki H, Yoshinaga K, Kondo T, Imai Y, Shiseki M, Mori N, Teramura M, Motoji T. 2014. Donor cell-derived leukemia after cord blood transplantation and a review of the literature: differences between cord blood and BM as the transplant source. *Bone Marrow Transplant* **49:** 102–109.

Smith KA, Cowell IG, Zhang Y, Sondka Z, Austin CA. 2014. The role of topoisomerase II beta on breakage and proximity of *RUNX1* to partner alleles *RUNX1T1* and *EVI1*. *Genes Chromosomes Cancer* **53:** 117–128.

Wang J, Mullighan CG, Easton J, Roberts S, Heatley SL, Ma J, Rusch MC, Chen K, Harris CC, Ding L, et al. 2011. CREST maps somatic structural variation in cancer genomes with base-pair resolution. *Nat Methods* **8:** 652–654.

Wiseman DH. 2011. Donor cell leukemia: a review. *Biol Blood Marrow Transplant* **17:** 771–789.

Yasuda T, Ueno T, Fukumura K, Yamato A, Ando M, Yamaguchi H, Soda M, Kawazu M, Sai E, Yamashita Y, et al. 2014. Leukemic evolution of donor-derived cells harboring *IDH2* and *DNMT3A* mutations after allogeneic stem cell transplantation. *Leukemia* **28:** 426–428.

Zhang J, Ding L, Holmfeldt L, Wu G, Heatley SL, Payne-Turner D, Easton J, Chen X, Wang J, Rusch M, et al. 2012. The genetic basis of early T-cell precursor acute lymphoblastic leukaemia. *Nature* **481:** 157–163.

Zhang J, Walsh MF, Wu G, Edmonson MN, Gruber TA, Easton J, Hedges D, Ma X, Zhou X, Yergeau DA, et al. 2015. Germline mutations in predisposition genes in pediatric cancer. *N Engl J Med* **373:** 2336–2346.